國立臺灣大學電機資訊學院資訊網路與多媒體研究所
碩士論文
Graduate Institute of Networking and Multimedia
College of Electrical Engineering and Computer Science
National Taiwan University
Master Thesis

設計三自由度旋轉觸覺提示以改進第一人稱視角體驗

TurnAhead: Designing 3-DoF Rotational Haptic Cues to Improve First-person Viewing (FPV) Experiences

柯柏丞
Bo-Cheng Ke

指導教授：陳彥仰博士
Advisor: Mike Y. Chen, Ph.D.

中華民國 112 年 7 月
July, 2023

doi:10.6342/NTU202303686

國立臺灣大學碩士學位論文
口試委員會審定書

TurnAhead：設計三自由度旋轉觸覺提示以改進第一人稱視角體驗

TurnAhead: Designing 3-DoF Rotational Haptic Cues to Improve First-person Viewing (FPV) Experiences

本論文係柯柏丞君（學號 R10944022）在國立臺灣大學資訊網路與多媒體研究所完成之碩士學位論文，於民國一百一十二年七月十二日承下列考試委員審查通過及口試及格，特此證明。

口試委員：

（簽名）

（指導教授）

所　長：

誌謝

首先，我要感謝我的指導教授，陳彥仰教授，讓我有幸成為人機互動實驗室的一員，並且在完成本篇論文的過程中給予很多意見和討論，並且付出極大的努力在完善本篇論文的架構，同時提供非常好的實驗室環境，設備齊全，機能完善。學長姐也樂於提供意見與正面回饋鼓舞自己，同屆同學與下一屆的學弟妹也在我遇到困難時提供幫助，不管是關於專案的雜事，抑或是生活中的大小事。

感謝旻翰在該專案剛起步時，與我熬過無數夜晚的腦力激盪與裝置實測，並總是彌補我在不擅長英文口說上的不足，不管是每一次專案課程上的進度報告，抑或是遠赴國際會議時的發表，舒緩我大部分的緊張與壓力。除此之外，後期儘管因為兵役無法密集參與專案，也非常妥善地完成 FPV 影片的分析工作，並且盡可能參與每一次討論時間，真的很感謝這一位自始自終陪伴我一起完成這個專案的二把手。

感謝陳譽在初期加入時就投入相當的參與度，快速跟上專案的當下進度並熱烈參與討論，時常提供精闢且關鍵的看法。除此之外，包攬了整篇論文的美術設計，近乎大部分的論文圖片與展示影片的製作都花費了很多心力。做事時的細心仔細與和我相當契合的做事風格，都讓我在推進這個專案時，有著非常好的協助力，也感謝陳譽在每一次討論結束後，都會花費不少時間和我閒聊並聆聽我的嘮叨。

感謝家宇分擔部分實驗場景的程式碼撰寫，並時常在離開實驗室以後，聊聊一些雜事並分享自己的煩惱，讓我在煩悶的研究生活中有很好的發洩窗口。感謝巧如主動加入我的專題，並以非常高的效率完成指派下去的任務，包含 2D 影片的場景設計與部分論文圖片和影片製

doi:10.6342/NTU202303686

作等。感謝舜昱提供攝影層面的協助，並且對於整篇論文的美術設計上給了很多的建議。感謝陳譽、家宇、巧如擔任實驗人員協助完成實驗，才能讓這篇足足有 4 個實驗的論文能夠在投稿死線前完成。

感謝過程中所有協助這個專案的專題生，還有參與實驗的受試者們，給予很多有幫助的建議與回饋。感謝所有在投稿 CHI 時的 reviewer 們，不吝給予本篇論文正面的評價與明確的改進方向。感謝遠赴德國參與國際論壇時同行的旻翰、陳譽、宇承、家宇和舜昱，讓我能夠在近乎無法進行英語口說的情況下，體驗了一次非常令人印象深刻且有趣的歐洲之旅。

感謝口試委員鄭龍磻教授、陳炳宇教授、余能豪教授和蔡欣叡教授，在學位考試時對報告和論文提出專業的問題，讓我對於自己的論文有更多反思和更深入的探討。感謝在我剛加入實驗時給予我初步研究理解的雋淼學長。感謝青邑學長讓我參與多個專案，對於研究透徹的解析讓我收穫良多，並時常給予關心。感謝琮珉、筠庭、柏佑和詩芩學長姐，在我研究上遇到困難時給予及時的幫助與討論。

感謝我的母親與兩個妹妹，在背後給我最大的支持，讓我能夠專注在實驗室的研究生活，並且給予我隨時可以回去的避風港，真的非常感謝。感謝從大學交識至今的柏瑋，在研究所共同修課並組隊，彼此幫助在學業上的煩惱。

此碩士學位論文之大部分研究成果同時發表於人機互動領域頂尖會議—計算機人機介面會議 ACM CHI 2023，TurnAhead: Designing 3-DoF Rotational Haptic Cues to Improve First-person Viewing (FPV) Experiences [15]，並榮獲該會議榮譽提名獎 Honorable Mention Award。

doi:10.6342/NTU202303686

摘要

「第一人稱視角（FPV）無人機」是最近發展起來的無人機種類，能夠進行精確地飛行並且捕捉以往難以捕捉的精采視覺體驗，例如穿越狹窄的室內空間和極近的接觸表面上飛行。FPV 視覺體驗雖然令人興奮，但通常會有頻繁的旋轉，可能導致受試者有不適感。因此，我們提出了「TurnAhead」，它使用對應鏡頭旋轉的 3 自由度（3-DoF）旋轉觸覺提示，以提高 FPV 體驗的舒適度、沉浸感和有趣度。它使用頭戴式附載空氣噴射裝置提供旋轉力回饋，是首個支持所有旋轉軸（偏航、俯仰和翻滾）旋轉的設備。我們進行了一系列的感知和形成性研究，探索觸覺提示的時間點和強度的設計，隨後進行了用戶體驗評估，共有 44 名參與者（四個實驗分別為 12, 8, 6, 18 人）。結果顯示，「TurnAhead」顯著改善了整體舒適度、沉浸感和有趣度，並且有 89％的受試者偏好使用它。

關鍵字：使用者體驗設計；觸覺回饋裝置；空壓噴氣；虛擬實境；第一人稱視角影片

doi:10.6342/NTU202303686

Abstract

First-Person View (FPV) drone is a recently developed category of drones designed for precision flying and for capturing exhilarating experiences that could not be captured before, such as navigating through tight indoor spaces and flying extremely close to subjects of interest. FPV viewing experiences, while exhilarating, typically have frequent rotations that can lead to visually induced discomfort. We present TurnAhead, which uses 3-DoF rotational haptic cues that correspond to camera rotations to improve the comfort, immersion, and enjoyment of FPV experiences. It uses headset-mounted air jets to provide ungrounded rotational forces and is the first device to support rotation around all 3 axes: yaw, pitch, and roll. We conducted a series of perception and formative studies to explore the design space of timing and intensity of haptic cues, followed by user experience evaluation, for a combined total of 44 participants (n=12, 8, 6, 18). Results showed that TurnAhead significantly improved overall comfort, immersion, and enjoyment, and was preferred by 89% of participants.

Keywords: User Experience Design; Haptic Device; Compressed Air Jet; Virtual Reality; First-person Viewing Video

doi:10.6342/NTU202303686

Contents

doi:10.6342/NTU202303686

doi:10.6342/NTU202303686

doi:10.6342/NTU202303686

List of Figures

doi:10.6342/NTU202303686

doi:10.6342/NTU202303686

doi:10.6342/NTU202303686

List of Tables

doi:10.6342/NTU202303686

Chapter 1

Introduction

First-person view (FPV) drone is a recently developed category of drones designed for precision flying and for capturing immersive and exhilarating viewing experiences. They are piloted using low-latency FPV goggles for high maneuverability, providing viewers with a bird-like flying experience that simply could not be captured before and are increasingly being used in blockbuster movie production. For example, FPV drones have enabled viewers to fly under and in-between robots that are assembling a Tesla car throughout a factory [35], and enable viewers to experience a car chase by flying under and through cars, bridges, and buildings [25].

As FPV footage becomes increasingly popular in movies, commercials, and social media, the largest drone manufacturer, DJI, recently launched its first two models of consumer FPV drones in 2021 and 2022. These ready-to-fly models have made FPV drones accessible beyond a small but vibrant DIY community, and have further accelerated FPV content creation. However, while FPV footage is exhilarating, current viewing experience does not provide any haptic feedback to enhance the experience. Furthermore, the camera motion, especially rotation, can lead to visually induced discomfort [16].

We present TurnAhead, which uses rotational haptic cues in 3-DoF (degrees of freedom) to improve the comfort, immersion, and enjoyment of first-person viewing (FPV) experiences. It uses headset-mounted air jets to provide ungrounded rotational forces that corresponds to camera rotation in 3 axes: pitch, roll, and yaw. TurnAhead is inspired by our prior system, HeadBlaster [19], which used air jets to provide lateral force feedback

doi:10.6342/NTU202303686

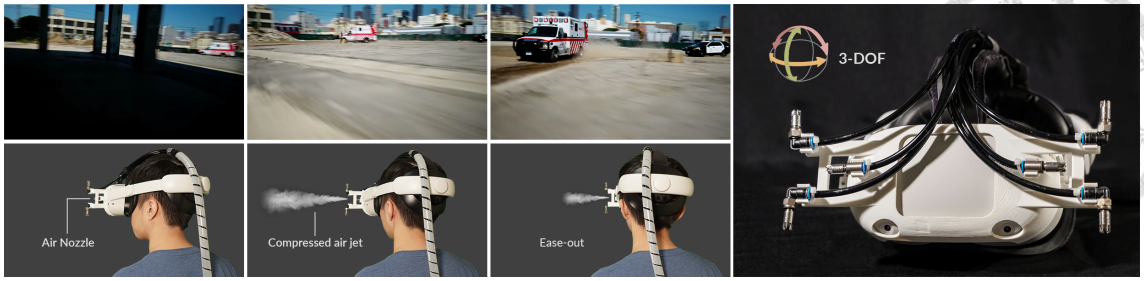

Figure 1.1: (a) TurnAhead explores the design space of applying 3-DoF rotational haptic cues to the head to improve comfort, immersion, and enjoyment of first-person viewing (FPV) experiences. In this example, a user is viewing a car chase scene from the movie Ambulance (2022) shot by FPV drones [25] as the camera rotates to the right; (b) Our device consists of 6 air nozzles that are mounted on the front of VR headset and placed tangent to the head, and is the first wearable device capable of generating rotational forces to turn left/right (yaw axis) that is in 84% of the rotations in FPV footage.

in 2-DoF for motion simulation. Because turning left/right (yaw) is the most common rotation axis for FPV, yet not supported by HeadBlaster's design, we iteratively developed new nozzle layouts to create the first wearable device to provide rotational forces in 3-DoF, as shown in Figure 1.1.

In particular, TurnAhead's nozzles are placed to generate forces *tangent* to the head, which is perceived as *shear* [37] and rotational forces; whereas HeadBlaster places nozzles to generate horizontal forces *perpendicular* to the skin, which are perceived as pressure and as lateral, translational forces. Additionally, we explored and evaluated haptic cue designs through a series of perceptual threshold and haptic cue design studies to design the timing and intensity of haptic cues, with a combined total of 44 participants.

To explore the design space, we first conducted a perception threshold study (n=12) to model how rotational cue intensity and duration affect recognition rate. Based on these findings, we then explored the haptic force curve and timing through two smaller-scale formative studies (n=8, 6), to inform cue designs that convey the speed, angle, axes, and timing of view rotations.

To evaluate the user experience of TurnAhead, we conducted an 18-person study to compare the baseline viewing experience with two haptic timing designs: *onset* and *anticipatory*, with the former providing haptic cue at the same starting time as rotation and the latter providing haptic cues *prior* to rotation. Results showed that both timing designs

doi:10.6342/NTU202303686

of TurnAhead significantly improved overall comfort, immersion, and enjoyment ($p < .01$) with large effect sizes. In terms of overall preference, 89% of participants preferred TurnAhead, and among them, the timing preference was evenly split with 48% preferring onset and 52% preferring anticipatory.

The rest of the paper is structured as follows: we first present our quantitative analysis of top FPV videos in terms of rotation speed, angle, axes, and frequency, which formed the basis of our design exploration, formative studies, and evaluation study. We then discuss our work in context of prior work, then present our device design and implementation. We describe our design exploration through a perceptual study, two smaller-scale formative studies, and a user evaluation study. Last, we discuss observations and limitations.

doi:10.6342/NTU202303686

Chapter 2

Background of FPV Drones and Analysis of Top FPV Videos

2.1 Background of FPV Drones and Video Categories

The first consumer quadcopter drone, Parrot AR.Drone 1.0, was launched in 2010. It was capable of live streaming QVGA (320x240) video over Wi-Fi to smartphones. By 2016, consumer drones are equipped with computer-vision technologies for obstacle avoidance and gimbals with intelligent subject tracking, designed for stable flights and cinematic video capture.

Flight enthusiasts have been pushing the boundaries of maneuverability by developing DIY FPV goggles and high-speed drones for racing, aerial tricks, and have produced a variety of viral FPV videos. Compared to non-FPV drones that use 2- or 3-DoF gimbals to provide stabilized footage with horizontal horizon, FPV drones have no gimbals or only single-axis gimbals that allows rotation around roll and yaw with optional pitch stabilization, making rotation around roll a unique signature of FPV footage.

Recognizing the growing popularity of FPV content, the largest drone manufacturer, DJI, launched its first ready-to-fly FPV drone with a top speed of 140km/hr in 2021. To make FPV even more accessible to novices and for indoor flights, DJI launched a smaller cinewhoop-style FPV drone, Avata, in 2022. It has built-in propeller guards to improve

doi:10.6342/NTU202303686

crash protection and safety around people, and a joystick-like motion controller that allowed novices to fly FPV without requiring several hours of simulator practice.

Figure 2.1: Example screenshots from two of the top 30 FPV videos that we analyzed: (Top) flying through the window of a high-speed, moving car [26]; and (Bottom) flying through a shopping mall and in and out of stores [4].

FPV drones have been specialized for racing, freestyle, and for capturing cinematic content, and their videos can be generally categorized into the following 4 key categories:

- **Racing**: footage from FPV races performing high-speed maneuvers.
- **Freestyle**: showcasing technical flying skills, such as flips, spins, and through tight openings, often for freestyle competitions.
- **Pursuit**: chasing and tracking specific moving subjects, such as a car chase at 140Km/hr and a mountain biker racing down a winding forest trail.
- **Cinematic**: immersive, bird-like flying experience throughout a scene, venue, and environment, such as winding through the insides of a bowling alley and diving down the face of a waterfall.

2.2 Analysis of Rotation Speed, Angle, Axes, Duration, and Frequency of FPV Videos

In order to characterize FPV viewing experiences to inform our design process and user experience evaluation, we analyzed popular videos in terms of rotation speed, angle, axes, duration, and frequency. The scope of this work is to design for popular FPV video viewing experience, rather than all possible videos, thus our video analysis focuses on content

doi:10.6342/NTU202303686

that are intended to be viewed by the general audience, rather than the more specialized footage from races and for freestyle competitions.

We surveyed and selected a total of 30 of the most popular FPV videos from Youtube and AirVūz [13], which is the top video sharing site specifically for drone videos. Specifically, for Youtube, we searched by the keyword ”FPV” and ranked by view count, and for AirVūz that has categorized videos, we selected top videos across the ”Cinematic FPV”, ”Cinewhoops”, ”Car chasing by FPV” and ”FPV Flythroughs” categories. The complete list of 30 videos are listed Table 1 in Appendices, and example screenshots from two of these videos are shown in Figure 2.1.

In order to analyze these videos in terms of rotation speed, angle, axes, and duration, we first attempted using computer-vision tools to do automated analysis. However, because most tools required either additional sensor and depth data (e.g. IMU and depth maps from LIDAR and stereoscopic cameras) or are trained on relatively stable videos (e.g. self-driving cars), these tools worked poorly for FPV videos which have frequent and fast rotations.

Therefore, we manually analyze and label these videos. We labeled rotations independently by each of the roll, pitch, and yaw axes in terms of angle and timing, rounded to the nearest multiples of 15 degrees. This approach captures both single-axis and multi-axis rotations, and captures rotations for which the starting and ending times for each axis may not fully overlap. For example, a rotation may start as single-axis (e.g. yaw), then later become multi-axis rotation (e.g. yaw + roll). Overall, a team of two people independently analyzed 79m:15s of FPV video, which took more than 40 person-hours at a analysis rate of about 30 minutes per 1 minute of video, including discussions to resolve differences in initial labeling.

Quantitative Results

Figure 2.2 shows the distribution of rotation time by axes, as percentages of the total rotation time. Single-axis rotation (76%) is the most common followed by two-axis (21%) and three-axis (4%) rotations. Overall, the most common rotation type is single-axis yaw

doi:10.6342/NTU202303686

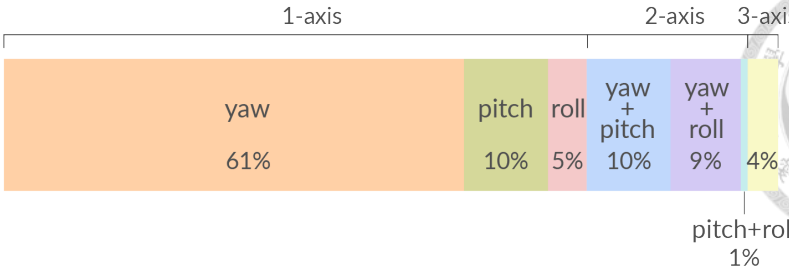

Figure 2.2: Distribution of rotation time by axes.

rotation at 61%. Furthermore, the most common rotation axis is yaw, with 84% of all rotations having yaw as one of its rotation axes.

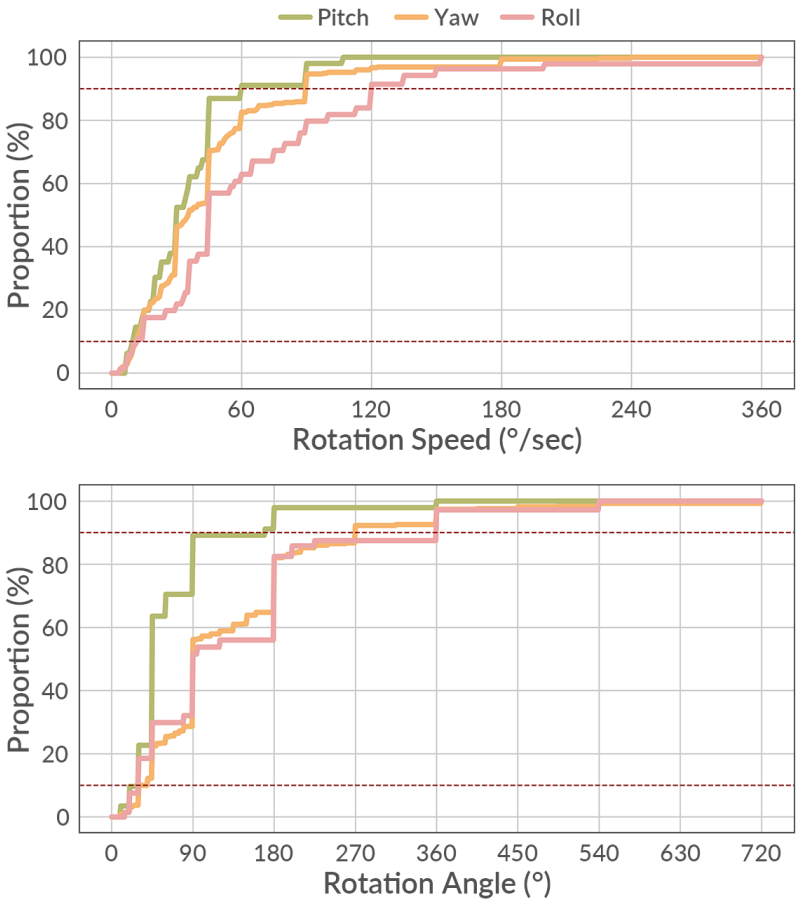

Figure 2.3: Empirical cumulative distribution functions (eCDF) of rotation speed and rotation angle by each of the 3 axes, with dotted red horizontal lines indicating the 10th and 90th percentiles.

Figure 2.3 shows the empirical cumulative distribution functions of rotational speed and angle by each of the 3 axes. We will use these results in our design process and user experience evaluation. For example, using the 90th- and 10th-percentile values as the upper-bound and lower-bound of rotational speed and angle.

doi:10.6342/NTU202303686

Chapter 3

Related Work

Our device and haptic designs are inspired by the following prior work on head-mounted haptic systems and air propulsion-based haptics.

3.1 Head-mounted Haptic Feedback

HeadBlaster [19] and Odin's Helmet [12] create ungrounded 2-DoF translational force feedback to the head for 2-DoF motion simulation (i.e. front/back, left/right) using air-propulsion jets and propellers, respectively. Watanabe et. al [39] used 4 propellers to create rotation in 2-DoF, yaw and pitch, and translation in 1-DoF (front/back). While air jet-based approaches require a compressed air source compressor and tubing, it is lighter, more compact, less noisy (70-80dB [19] vs. 100dB [12, 39]), and more responsive than propeller-based approaches (20ms [38] vs. 300ms-500ms [11, 39]).

GyroVR uses headset-mounted spinning flywheels to create resistive force to simulate inertial forces [9]. Electrical head actuation [34] uses electrical-muscle-stimulation (EMS) of the neck muscles to turn the head in 2-DoF around its yaw (left/right) and pitch (up/down) axis.

FacePush [3] generates normal force on the face for haptic feedback. They demonstrated 1-DoF guidance in 360° video. HangerOVER [17] utilizes the Hanger Reflex phenomenon, an involuntarily head rotation about only the yaw-axis due to pressure applied around the head; however, this reflex is not present on some users and the effect is impre-

doi:10.6342/NTU202303686

cise.

While prior approaches explored 1-DoF and 2-DoF translational and rotational feedback, FPV experiences rotate in all 3 DoFs, which motivated the development of our device that is capable of rotation in all 3 axes. In particular, rotation around roll is a key signature of FPV footage that is in 19% of rotations. While the lateral forces applied to the head by HeadBlaster and Odin's Helmet cause both translation and tilt in pitch and roll, their designs do not support the most common (84%) rotation for FPV, yaw.

3.2 Air Propulsion-based Haptics

Ungrounded air propulsion forces can be generated using compressed air jets [10, 36, 19, 28] and high-speed propellers [11, 12, 14, 30, 39]. The key benefit of propellers is that it can be powered by batteries, whereas air jet systems require compressed air sources, either portable air tanks or air compressors. We selected air jets for TurnAhead because it offers several key performance benefits for our use case: 1) significantly faster response time and lower latency, on the order of 20ms [38] vs. 300-500ms [11, 39]; 2) significantly lighter head-mounted weight and compact size; and 3) significantly lower noise, 70-80dB vs. 100dB for head-mounted air jets [19] vs. propellers [12, 39].

3.3 Visuo-Vestibular Recoupling to Improve Comfort

There have been several approaches that physically stimulate the vestibular system to reduce discomfort and sickness in VR. Bone-conductive vibration (BCV) actuates bone-conducted transducers near the ears during view rotation in VR to reduce sickness, but its vibration frequency is audible and can be uncomfortable to users [40, 41]. Furthermore, the stimulation is *fuzzy* in that it does not provide information on the direction of rotation. Other approaches provide stimulation during locomotion in VR, such as walking by physically striking near the ears [20] and unobtrusive vibration behind the ears [24] during each footstep.

Galvanic vestibular stimulation (GVS) applies electric current via electrodes around

doi:10.6342/NTU202303686

the mastoid part, and is capable of making the body sway about three axis, although precise control remains challenging due to differences between people [1, 7, 22, 31, 41]. However, GVS can cause significant discomfort for some users, such as experienced mild to moderate pain (91%), general discomfort (55%), and headache (36%) [18].

Compared to the above approaches that provide stimulation during motion/rotation events, we also explore the design of anticipatory cues that are provided prior to rotation, to help users anticipate upcoming view rotation.

doi:10.6342/NTU202303686

Chapter 4

system design, implementation, and validation

Our system design is inspired by HeadBlaster [19], which provides ungrounded force feedback via headset-mounted air jets. While HeadBlaster provides lateral forces in 2-DoF, we designed our device to provide rotational forces in 3-DoF. We have open-sourced the entire system, including the 3D models of nozzle mounts, electronic schematics, Arduino code, and control software written in C#.[1]

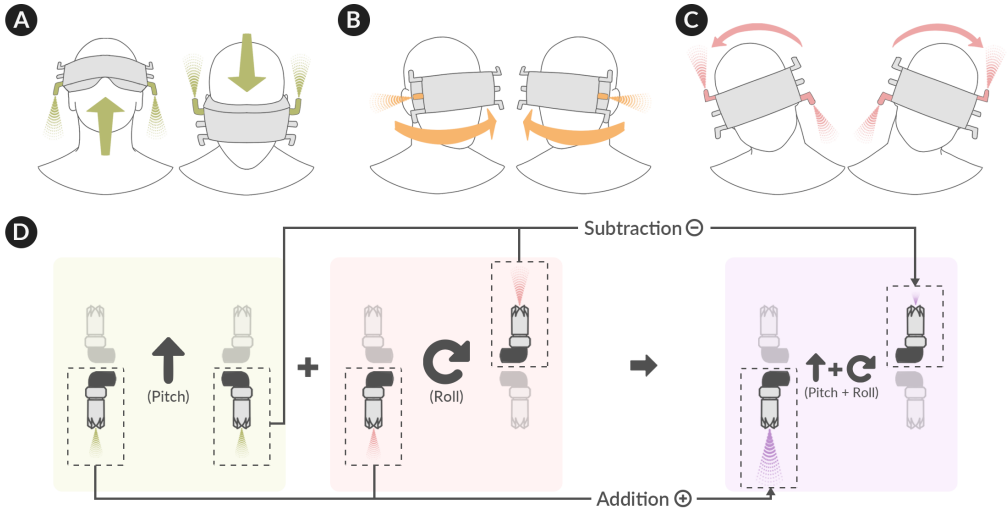

Figure 4.1: Nozzles activated for single-axis rotation: (a) pitch, (b) yaw, and (c) roll; (d) Force *addition* and force *subtraction* calculation for multi-axis rotation that share nozzles and use opposing nozzles, respectively.

[1]Open Source URL: https://github.com/ntu-hci-lab/TurnAhead

doi:10.6342/NTU202303686

4.1 Wearable Design

To keep the device light and easy to mount, we designed 3D-printed nozzle mounts that attach to the front of the VR headset. Our first prototype used 10 nozzles mounted on the Vive Pro headset, shown in Figure 4.2(c), and based on user feedback, we reduced complexity and weight of the design to use 6 nozzles on the Meta Quest 2 VR headset, as shown in Figure 1.1(b).

The wearable device, including 6 x Silvent 1001 noise-reducing nozzles, fittings, and headset mount, weighs 102g (excluding tubing). The extended 250cm x 6 tubings from the air compressor weigh a total of 240g, which can supported by a backpack or be supported externally so that the weight is no felt on the head (e.g. suspended from the ceiling or supported by the headset of a chair).

To generate rotational cues for each single axis, the corresponding nozzles to activate are shown in Figure 4.1(a)(b)(c). For multi-axis rotation, specifically pitch and roll, there are two possible types of nozzle conflicts: 1) two rotations requiring the use of the same nozzle, and 2) two opposing nozzles being activated at the same time, canceling out their forces. We optimize nozzle and air usage by using force *addition* and force *subtraction* to address these, respectively, with an example shown in Figure 4.1(d).

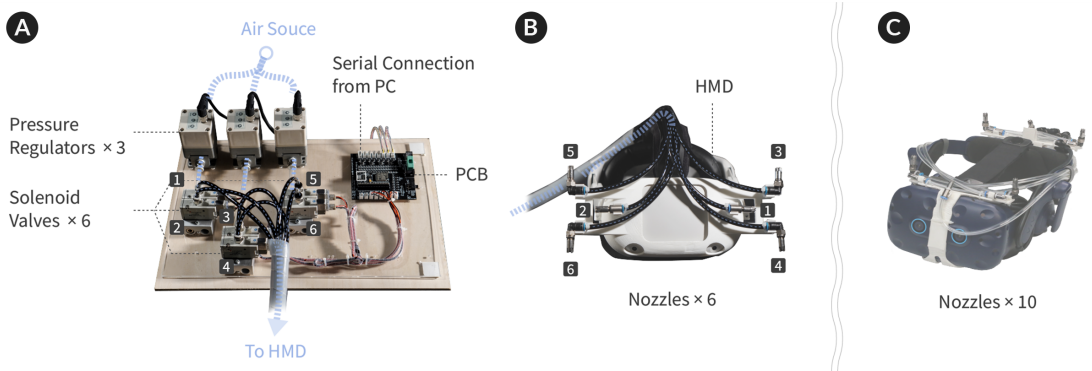

Figure 4.2: (a) The pneumatic control system; (b) Current (V2) version of the headset mount with 6 nozzles; (c) V1 version of our prototype that used 10 nozzles.

doi:10.6342/NTU202303686

4.2 Pneumatic Control

Figure 4.2 shows the pneumatic control system and the corresponding nozzles. Three electro-pneumatic pressure regulators (SMC ITV2050) control force magnitude and six solenoid valves (SMC SYJ712) control the direction of forces. Compressed air is supplied via tubing 6mm in diameter, and 250cm in length from a FIAC 5HP soundproof air compressor, with a rated operating noise of 65dB measured at 1 meter.

4.3 Force Magnitude

To measure force magnitude, we attached a nozzle to an L-Shape fitting model and mounted it on an IMADA ZTS20N load cell, which can record data at 2000Hz at up to 20N and has an accuracy rating of 0.2% full scale (0.04N). We measured the force magnitude at pressure increments of 50kPa, over the operating pressure range from 100-600kPa, with tubing 6mm in diameter and 250cm in length. Figure 4.3 shows the linear relationship between force magnitude and air pressure.

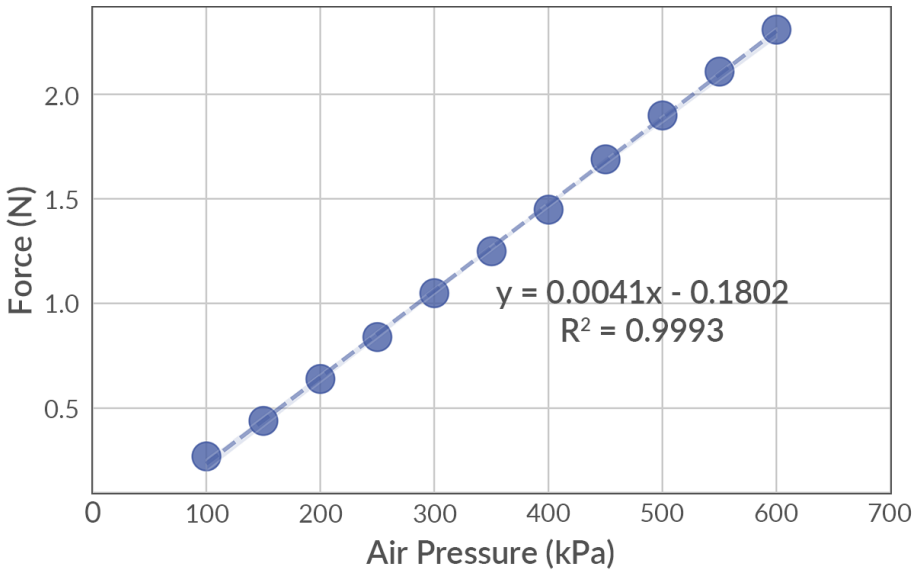

Figure 4.3: Linear regression of force magnitude vs. air pressure.

doi:10.6342/NTU202303686

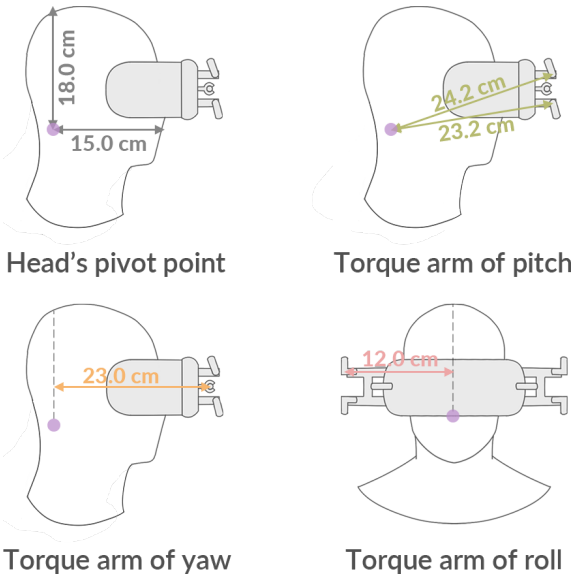

Figure 4.4: Average human head's pivot point, and torque arm measurements from the pivot point to nozzle locations for each axis.

4.4 Torque Arm Lengths and Torque Calculation

Relative to the pivot point of the head, different nozzles will have different torque arm lengths. According to Yip et al. [42], the human head's pivot point is shown in Figure 4.4, and we show the torque arm lengths for the nozzles for each axis using the average size of the head. The torque for each axis can then be calculated by multiplying force magnitude and torque arm length.

4.5 Actuation Latency

The actuation time of a haptic system measures the time between when a haptic command is sent to the system and when force feedback begins. In a compressed air-based system, this latency is primarily due to the time it takes pressure regulators to control the pressure, solenoid valves to physically open, and compressed air to flow to the nozzle. We measured the actuation latency by connecting the IMADA ZTS20N load cell, which samples at 2000Hz, to a PC and calculating the time between the PC sending an actuation signal and the PC reading the corresponding load cell measurement, and then repeating the process 100 times. The average latency from a Unity 3D API call to actuation is about 52ms. Therefore, we start the actuation 52ms in advance to correct the latency.

doi:10.6342/NTU202303686

4.6 Noise

We measured the nozzle noise by placing a decibel meter (WS1361C) at a distance of 1 meter. The noise level is highest at 73dB when actuating at the maximum pressure of 600kPa. In actual usage, the maximum pressure does not exceed 300kPa, and the noise level is less than 67dB. To put this noise level in context, HeadBlaster [19] reported that their 80dB noise could be effectively mitigated by using active noise-canceling headphones and sounds from the virtual experiences, such that it was not noticeable to users. In addition, according to the Centers for Disease Control and Prevention (CDC), USA, the noise level of 67dB is between the 60dB of ”Normal conversation, air conditioner” and 70dB of ”washing machine, dishwasher”.

doi:10.6342/NTU202303686

Chapter 5

Study #1: Directional Cue Recognition Threshold

To understand the minimum duration and intensity of haptic cues that can be perceived and correctly recognized by users, we conducted a perception study on recognition accuracy vs. cue duration and intensity.

5.1 Study Design

The study design is based on the constant stimuli methodology of psychophysical studies [21], which determines a threshold by presenting an observer with a set of stimuli of which some are above and below the threshold in a random order.

In this study, haptic cues with different intensity, duration, and direction are presented to the users in random order, and participants are asked to report a recognized direction or unknown (i.e. no forced choices). Based on a 4-person pilot study, we selected five different intensities of torques and five different duration that when combined, range from below recognition threshold (but above detection threshold) to above recognition threshold. The 5 intensities (i.e. torque) are: 2, 4, 6, 8, and $10N{\cdot}cm$ and the 5 durations are: 100, 150, 200, 250, and 300ms. We enumerated all possible combination with 6 rotational directions, for a total of $5 \times 5 \times 6 = 150$ conditions, randomly shuffled and the set of 150 conditions were repeated twice for 300 total trials per participant.

doi:10.6342/NTU202303686

5.2 Study Procedure

Participants first put on a Meta Quest 2 VR headset with our device, and were presented with practice haptic cues in all 6 rotational directions to become familiar and comfortable with the setup and process. Because no visual feedback was used, the VR headset was powered off. Noise-canceling headphones playing white noise were used to avoid extrinsic factors that would influence their judgement. After each cue was presented, participants verbally indicated the recognized direction or unknown if they are not certain. The cue could be repeated as requested by participants.

Participants would complete the 150-condition set twice, with a 5-minute break in between. After completing the second set, we conducted semi-structured interviews on how participants recognized the directions, how they ranked the ease of recognizing directions for the 3 axes, and any open-ended feedback. The entire study took an average of 35 minutes to complete.

5.3 Participants

We recruited 12 participants, 10 males and 2 females with age 21 to 27 (mean = 23.0, SD = 2.0), with Motion Sickness Susceptibility Questionnaire (MSSQ) score from 5.61 to 114.3 (mean = 49.6, SD = 32.7), which corresponds to 6th to 94th percentile [8]. Among participants' prior experience with VR, 7 had used VR more than once in the last three months, 2 about once a year, and 3 never. For participants' prior experience with FPV videos, 6 had watched FPV videos more than once in the last month, 5 about once a year, and 1 never. The participants received a nominal compensation for their participation.

5.4 Results and Discussion

Figure 5.1 shows line charts of the percentage of participants that correctly recognized the haptic cue direction (for both trials) vs. duration and torque, for all 6 rotational directions. For completeness, we also provide the line charts for the percentage of participants that

doi:10.6342/NTU202303686

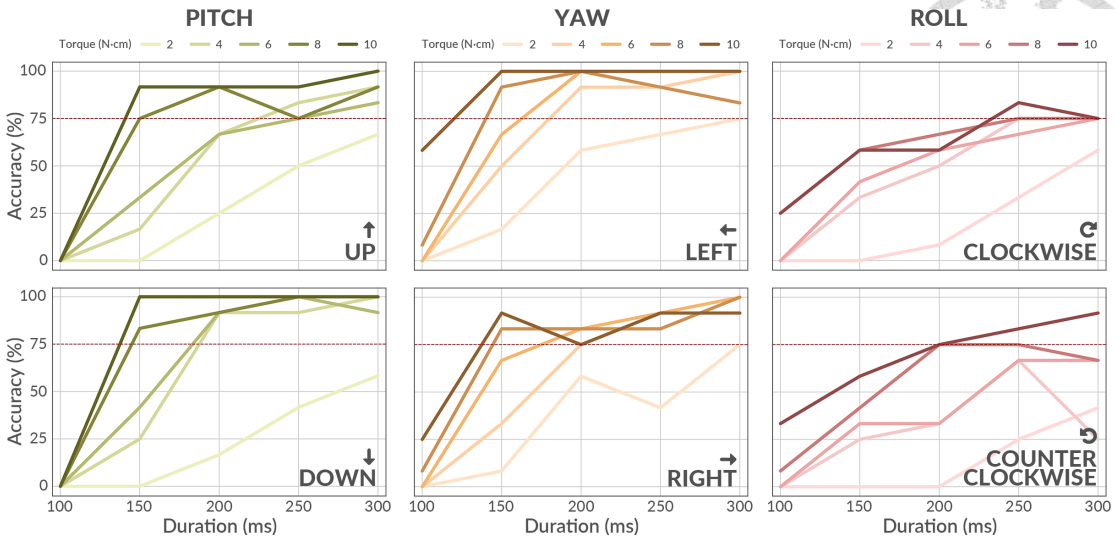

Figure 5.1: Percentage of participants that correctly recognized the haptic cue direction (for both trials) vs. feedback duration and torque, for each of the 6 directions. The 5 lines in each chart are colored from light to dark to represent increase in torque. Horizontal red dotted lines indicate 75th-percentile accuracy (i.e. 75% recognition threshold).

recognized correctly in at least one of the two trials in Appendix 10.

The results show the following trends:

- Recognition accuracy increases as duration increases, and as torque increases.
- Recognition accuracy is symmetrical about each axis. for example, the two directions around the pitch axis, i.e. up and down, have similar accuracy.
- *Roll* axis has lower recognition accuracy, while *pitch* and *yaw* have similar accuracy.

In psychophysical threshold studies, detection thresholds are typically defined as 50% correct performance for yes-no rating experiments and 75% for 2-AFC experiments, although these definitions are somewhat arbitrary and some authors define detection thresholds using different values, such as 68% [21, 6]. For our purpose of designing directional haptic cues recognizable by most participants, we use the higher threshold of 75%.

Based on the study results, for at least 75% of participants to correctly recognize cue directions in all directions, the minimum duration is 250ms with torque: $4N{\cdot}cm$ in *pitch* and *yaw* directions, and $8N{\cdot}cm$ in *roll*. We will use these torque values as the minimum *Recognition Threshold* in subsequent feedback designs.

doi:10.6342/NTU202303686

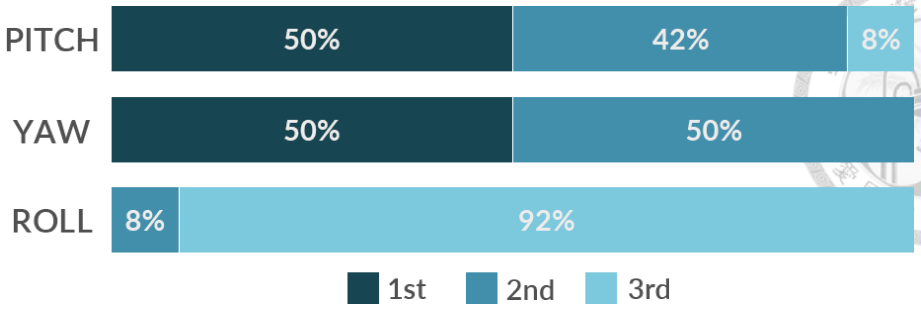

Figure 5.2: Distribution of *ease of recognition* ranking for each axis.

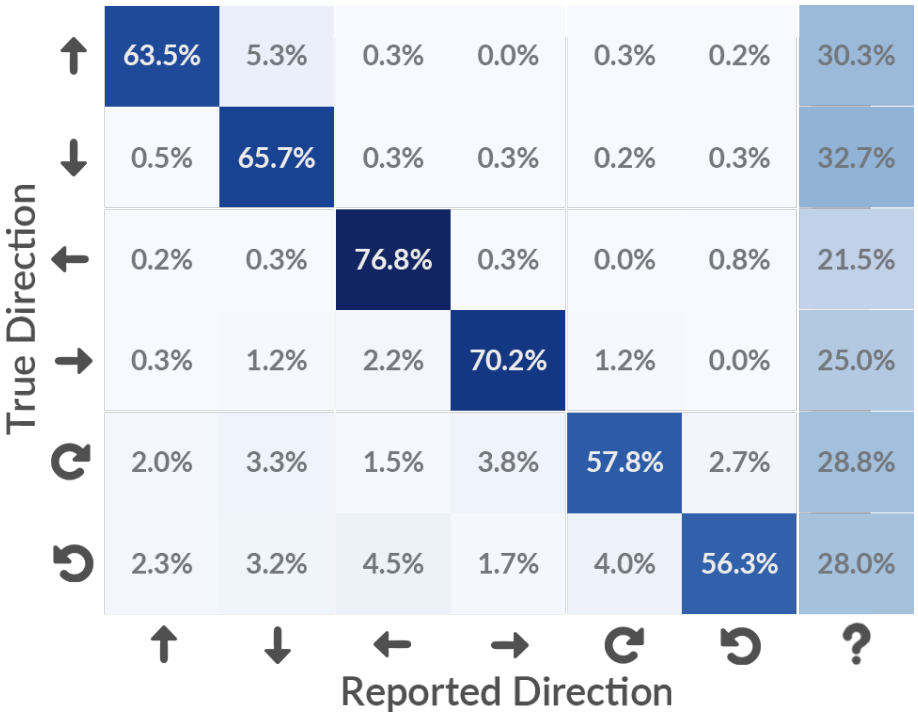

Figure 5.3: Confusion matrix of the direction recognition study results.

Figure 5.2 shows participants' subjective ranking of ease of recognition for the 3 axes. The ranking results are consistent with the accuracy analysis that rotations around *pitch* and *yaw* are similarly easy to recognize, while rotations around *roll* are significantly more difficult to recognize. Figure 5.3 shows the distribution of recognition errors using a confusion matrix, showing no clear confusion between two stimulus directions and that participants reported unknown rather than guessing the directions.

Qualitative Feedback

We observed minimal head rotation throughout the study including at the strongest torque and longest duration. Participants reported that the stronger cues can easily be recog-

doi:10.6342/NTU202303686

nized, except 2 participants reported that the roll axis was difficult even at the largest torque setting (P5, P7). Two participants commented that they perceived different headset vibration patterns (P9, P11) and slight lifting of the headset cushion (P6, P9) depending on the nozzles being actuated. Some reported that turning right vs. clockwise, and left vs. counterclockwise were confusing (P0, P4, P7, P8, P10).

doi:10.6342/NTU202303686

Chapter 6

Study #2: Small Formative Design Study on Rotation Speed and Angle

6.1 Design Exploration

To explore feedback designs for rotational speed and angle, we conducted a small formative study to explore the design space. For rotational speed, we explored a design that scales feedback intensity (i.e. torque) linearly to rotational speed, which is inspired by HeadBlaster [19] and AirRacket's [36] designs that mapped feedback intensity linearly to motion sensation and impact force magnitude, respectively. Also, to help users sense the progress of the rotation, we explored a design that gradually decreases intensity, which is inspired by the *ease-out* technique commonly used in animation.

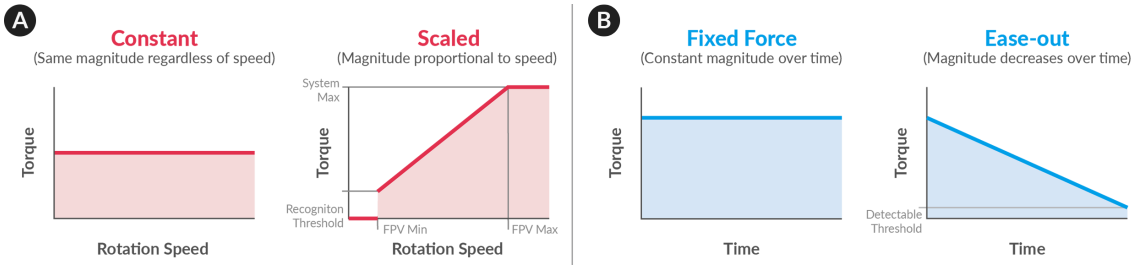

Figure 6.1: Intensity mapping designs: (a) between feedback intensity (i.e. torque) and rotational speed, showing constant feedback intensity regardless of rotation speed vs. linearly scaling of feedback intensity to rotation speed; (b) between feedback intensity and progression, for both fixed intensity throughout vs. easing-out throughout the rotation.

doi:10.6342/NTU202303686

We based the range of torque of the intensity mapping functions on actual FPV footage analysis data (Fig. 2.3). To eliminate the effects of outliers and extreme values, we used the 10th-percentile and 90th-percentile of the empirical cumulative distribution functions of rotation speed and angle as the *lower* and *upper* bounds in the mapping functions.

6.1.1 Scaling Intensity based on Rotation Speed

There are numerous approaches to designing torque mapping functions to rotational speed, each with its own set of trade-offs. We describe an example mapping function that preserves the dynamic range of rotational speed to minimize clipping by linearly mapping the range of rotational speed to the range of torque output above the *recognition threshold* for each axis. This ensures that all rotational cues, when provided, would be perceivable to users.

As shown in the Figure 6.1(a), based on the rotational speed within the common rotation speed range in FPV, torque is linearly scaled to the system max torque from the recognition threshold. If the rotation speed for an axis is below the lower bound (i.e. floor), no haptic cue will be provided. Conversely, if the rotation speed is above the upper bound (i.e. ceiling), the system max torque is provided. The lower bound helps reduce noise/jitter in view orientation, and the upper bound helps increase the actual dynamic range of feedback provided.

6.1.2 Easing-out based on Rotation Angle

We found it unsettling to keep pushing the head while the camera rotated, and there was no way of expecting when the rotation would end. To this, we designed a curve with a gradually decreasing force from the beginning to the end of the camera rotation. We can gain several advantages from this design, including the fact that the user does not have to constantly feel the force on the head and that we can effectively reduce the load of our device on the jet volume. In addition, the force drop may indicate the end of the view-point rotation to the user.

As shown in Figure 6.1(b), The starting force at the beginning, decided by the rota-

doi:10.6342/NTU202303686

tional speed, gradually decreases to detectable threshold as the camera rotates, ensuring that the user can feel the haptic feedback throughout the entire rotation.

Figure 6.2: Example VR 360 scenes used in Study 2 and 3, based on 3D environments: (Top) Flooded Grounds [32] and (Bottom) Sun Temple [33].

doi:10.6342/NTU202303686

6.2 Study Design and Procedure

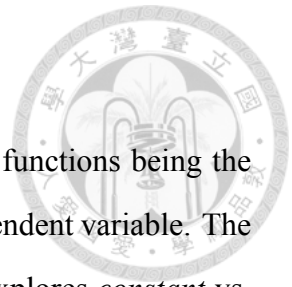

The study uses a within-subjects design with the intensity mapping functions being the independent variable and user preference and feedback being the dependent variable. The study is structured as two phases: 1) the first *rotation speed phase* explores *constant* vs. *scaled* torque based on rotation speed; and 2) the second *rotation angle phase* explores *fixed* torque vs. *ease-out*.

Participants used the Meta Quest 2 VR headset to navigate four different paths in VR scenes developed in Unity in first-person view (FPV) as shown in Figure 6.2. Passive navigation consisted of forward movement and random rotation about an axis, based on the rotation composition from our FPV video analysis (Sec. 2).

Participants experienced two paths in the first *rotation speed phase*: one using *constant* and the other *scaled* torque designs, in counterbalanced ordering. The second path mirrored the first path (i.e. reversed the starting and ending points), in order to have the exact composition of rotations and scenes, and to avoid users being able to predict the next turn. To explore more speeds, the composition of rotations for each path was three rotational speeds and two rotational angles (3×2) for each of the rotational axes, for a total of $3 \times 2 \times 3 = 18$ rotations.

Participants experience two paths in the second *rotation angle phase*: one with *ease-out* and the other with *fixed* torque designs, in counterbalanced ordering. To explore more angles, the composition of rotations for each path was two rotational speeds and three rotational angles (2×3) for each of the rotational axes, for a total of $2 \times 3 \times 3 = 18$ rotations. The second path is a mirrored version of the first path for the same reasons above.

After an introduction to the study and filling out Motion Sickness Susceptibility Questionnaire (MSSQ), participants went through a practice phase to become familiar with the VR environment and system, and experienced FPV with no force feedback for 30 seconds, followed by several random force feedback. Within each phase, each path took about 2 minutes to complete, with a 5-minute break between them. At the end of each phase, participants rated comfort and immersion of the two experiences on a 7-point Likert scale,

doi:10.6342/NTU202303686

reported their overall preference, and we conducted semi-structured interviews for qualitative feedback. For the second phase, participants additionally reported their preference for a more predictable rotation progression. The entire study took about 40 minutes to complete, including the initial introduction, MSSQ, practice phase, experiments, breaks, and interviews.

6.3 Participants

We recruited 8 participants, 6 males and 2 females with ages ranging from 16 to 23 (mean = 20.5, SD = 2.3), with Motion Sickness Susceptibility Questionnaire (MSSQ) scores ranging from 0 to 71.3 (mean = 19.4, SD = 29.9), which correspond to 0th to 61th percentile [8]. Among participants' prior experience with VR, 2 used VR more than once in the last three months, and 6 about once a year. The participants received a nominal compensation for their participation.

6.4 Results and Discussion

Rotational Speed: Constant vs. Scaled Feedback Intensity

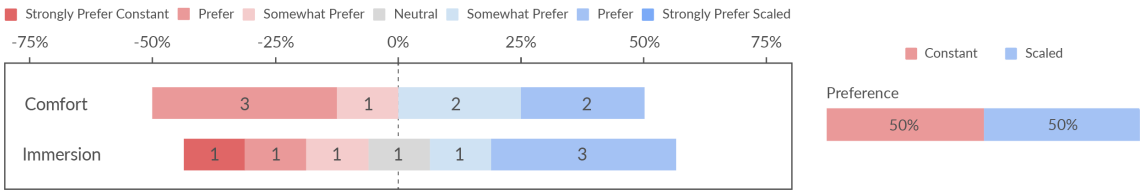

Figure 6.3: *Constant* vs. *Scaled* feedback design for rotation speed: (Left) comfort and immersion on a 7-point Likert scale; (Right) overall preference.

We observed small but noticeable head rotation for larger torque. Figure 6.3 shows even split in overall preference, and minimal difference in comfort and immersion.

Participants liked the scaled design because of better matching of the feedback intensity and camera rotation speed (P3, P6); however, some reported that the largest torque in the *scaled* design can sometimes be too strong for too long (P1, P2, P5). The *ease-out*

doi:10.6342/NTU202303686

design should help maintain the positive aspects of the scaled design, while mitigating its negative aspects.

Rotation Progress: Fixed vs. Ease-out Feedback Intensity

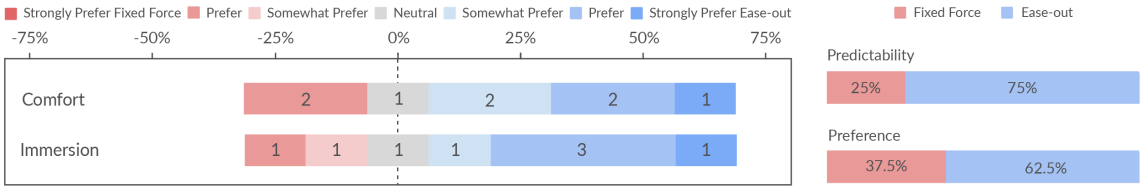

Figure 6.4: *Scaled + fixed* vs. *Scaled + ease-out* feedback design for rotation angle: (Left) comfort and immersion on a 7-point Likert scale; (Right) user preference on predictability and overall preference.

Figure 6.4 shows that participants preferred *ease-out* for comfort and immersion. 75% of participants found that the rotation angle to be more predictable with *ease-out*, and overall 62.5% preferred the *scaled + ease-out* design vs. *scaled + fixed* design.

Participants reported that at the end of the *fixed* condition, the torque stopped instantly causing an unexpected recoil/rebound effect, which was addressed by the *ease-out* design (P0, P4, P6). Some reported that the gradual decrease in force during the rotation helped with understanding the progression of rotation, which felt more realistic (P3, P7) and smoother (P0, P1).

doi:10.6342/NTU202303686

Chapter 7

Study #3: Small Formative Design Study on Timing

7.1 Design Exploration

Inspired by prior studies' observations that motion sickness is inversely related to the ability to anticipate future motion paths [5] (e.g. car drivers are less likely to get motion sickness than passengers [27]), we explore feedback timing designs that provide *anticipatory cue* prior to the view rotation.

We first experimented with timing designs by simply starting the force feedback prior to rotation. However, users reported that the force magnitude was too large which led to unexpected and confusing head rotation prior to view rotation, whereas our design goal was to provide a recognizable cue. Therefore, we added an additional force feedback phase, called the *anticipatory cue phase* prior to the view rotation phase, called the *turning phase*.

For the *turning phase*, the force feedback adopts the *scaled + ease-out* design from Study 2 (Sec. 6) that was most preferred by participants. As for the *anticipatory cue phase*, which aims to provide a minimally recognizable cue, we use the recognizable thresholds for torque and duration from Study 1 (Sec. 5): $4N{\cdot}cm$ for pitch/yaw and $8N{\cdot}cm$ for roll for 250ms or longer.

doi:10.6342/NTU202303686

7.2 Study Design and Procedure

The study uses a within-subjects design, with cue timing as the independent variable and user preference and feedback as dependent variable. Participants used the Meta Quest 2 VR headset to navigate VR scenes developed in Unity in first-person view (FPV) as shown in Figure 6.2.

Based on a 4-person pilot study, we selected three anticipatory timings to explore that ranged from barely noticeable to sometimes too long, which were 300, 600, and 900ms. We designed three distinct FPV paths that had the same rotation composition from our FPV video analysis (Sec. 2). For each path, there were three different rotational speeds and two different rotational angles for each of the rotational axes, for a total of $3 \times 2 \times 3 = 18$ rotations. The ordering of the paths and timing were counterbalanced.

After an introduction to the study and filling out Motion Sickness Susceptibility Questionnaire (MSSQ), participants went through a practice phase to become familiar with the VR environment and system, and experienced FPV with no force feedback for 30 seconds, followed by several random force feedback. Each path took about 2 minutes to complete, with a 5-minute break between them. At the end, participants reported their preference for comfort, immersion, predictability, and overall experience of the three experiences, and we conducted semi-structured interviews for qualitative feedback. The entire study took about 25 minutes to complete, including the initial introduction, MSSQ, practice phase, experiments, breaks, and interviews.

7.3 Participants

We recruited 6 participants, 5 males and 1 female with age ranging from 21 to 26 (mean = 23.2, SD = 1.7), and with Motion Sickness Susceptibility Questionnaire (MSSQ) scores ranging from 5.61 to 113.5 (mean = 52.6, SD = 47.4), which correspond to 6th to 93th percentile [8]. Among participants' prior experience with VR, 1 used VR more than once in the last 1 month, 5 about once a year. For participants' prior experience with FPV videos, 6 watched FPV videos more than once in the last 1 month. The participants received a

doi:10.6342/NTU202303686

nominal compensation for their participation.

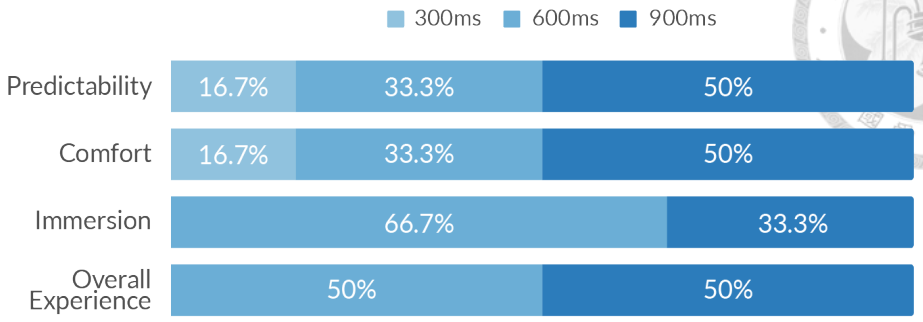

Figure 7.1: Most preferred anticipatory cue timing for predictability, comfort, immersion, and overall experience.

7.4 Results and Discussion

Figure 7.1 shows the distribution of the most preferred timing for predictability, comfort, immersion, and overall experience. Results show that the two longer anticipatory timings were preferred more for predictability of the next rotations as well as comfort, immersion, and the overall experience. The overall preference for 600ms and 900ms was even split at 50% each.

Qualitative Feedback

Participants reported that the feedback intensity of the *anticipatory cue phase* was noticeably different from the intensity of the *turning phase* (P0, P2, P3, P4), and found the early cue to be ”interesting” (P2) and ”appealing” (P3). In addition, half of the participants reported that: 1) 300ms was not perceived to be in advance of the rotation (P0, P2, P5); 2) 600ms and 900ms had little noticeable differences (P0, P1, P3); and 3) 900ms was too long at times with noticeable incongruity (P0, P2, P5).

doi:10.6342/NTU202303686

Chapter 8

Study #4: User Experience Evaluation

To evaluate the user experience of TurnAhead, we conducted a user study to compare: 1) *anticipatory* cue vs. 2) *onset* cue vs. 3) *no* cue as baseline. The cue force design used the *scaled* + *ease-out* design from Study 2 (Sec. 6) that was most preferred by participants. The anticipatory timing was selected to be 600ms, because even though 600ms and 900ms were preferred equally in Study 3 (Sec. 7), participants' qualitative feedback showed that while those who preferred 900ms reported similar experience with 600ms, those who preferred 600ms were uncomfortable with 900ms. The onset condition provides cue at the beginning of rotation.

8.1 Designing FPV Experience

In order to cover different FPV content type (ie. indoor vs. outdoor) and FPV viewing scenarios (ie. VR and 2D videos), we developed: 1) a VR environment with indoor and outdoor scenes and 2) selected popular indoor and outdoor FPV footage to be shown as 2D video via the HMD.

8.1.1 VR 360

Figure 8.1 shows example indoor and outdoor scenes from the VR environment we developed using Unity. To prevent users from remembering rotations from a repeated path, we created 3 distinct paths based on the rotation composition from our FPV video analysis

doi:10.6342/NTU202303686

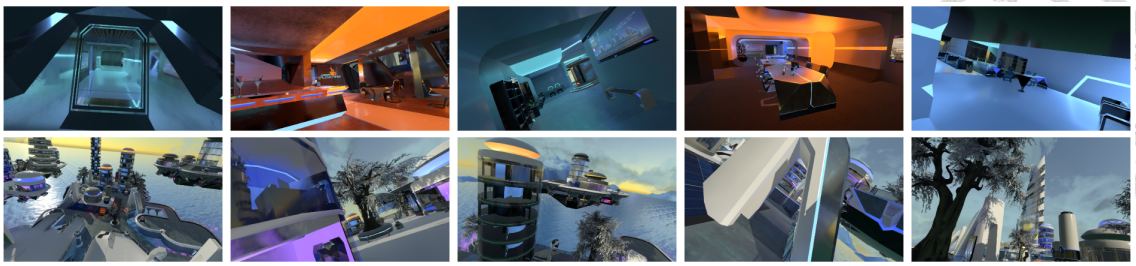

Figure 8.1: Example indoor scenes (top) and outdoor scenes (bottom) from the VR 360 environment used in Study 4, based on 3D Platform City [2].

(Sec. 2), in terms of rotational axis, speed, and angle. Each path consists of 10, 2, and 2 rotations around yaw, pitch, and roll axis, respectively, to approximate the composition from Figure 2.2, and the rotation speed and angle are uniformly sampled from their corresponding empirical cumulative distribution (Fig. 2.3). To make the paths appear more organic, small random rotations of 1-2 degree/sec about each axis were added to each turn. The duration of each FPV path is 1 minute.

8.1.2 2D Video

We grouped the videos from our FPV video analysis (Sec. 2) into indoor and outdoor footage. Indoor videos primarily fly through different rooms and indoor spaces, and consist of mostly yaw rotation, likely because of the lack of vertical space for pitch rotation and disorientation due to roll. Outdoor videos have more rotation in pitch and roll directions, but generally have more cuts to travel through a variety of landscapes at a faster tempo. In order to have 3 distinct videos that have similar visual, we identified 3 indoor videos flying through bowling alleys and 3 outdoor videos of landscape and buildings, and selected 1-minute segment from each that had similar rotation composition. To avoid cropping the videos while viewing, the 2D videos are anchored to the HMD, similar to personal home theater headsets.

doi:10.6342/NTU202303686

8.2 Study Design and Procedure

The study used within-subjects design, with the 3 cue conditions (anticipatory vs. onset vs. no cue) as the independent variable, and users' subjective ratings on comfort, immersion, enjoyment, and overall preference as the dependent variable. The 3 cue conditions were experienced for each of 3 scenario blocks: VR, indoor 2D video, outdoor 2D video, in counterbalanced ordering. The ordering of the 3 scenario blocks were also counterbalanced.

After an introduction to the study and filling out Motion Sickness Susceptibility Questionnaire (MSSQ), participants went through a practice phase to become familiar with the VR environment and system, and experienced force feedback in all 6 rotational directions. Each condition was one minute, followed by a one-minute break. After each condition, participants rated comfort, immersion, and enjoyment on a 7-point Likert scale. After each scenario block, participants reported their overall preference and reasoning, and took a 5-minute break. Additionally, participants were informed that they could take breaks at any time and also drop out at any time if they felt too uncomfortable. At the end of the study, we conducted semi-structured interviews for qualitative feedback. The entire study took about 60 minutes to complete.

8.3 Participants

We recruited 18 participants (9 male and 9 female) with age ranging from 20 to 45 (mean = 23.4, SD = 5.6), and with MSSQ score from 2.64 to 80.2 (mean = 32.2, SD = 22.0), which corresponds to 3rd to 86th percentile [8]. Among participants' prior experience with VR, 2 used VR more than once in the last three months, 8 about once a year, and 8 never. For participants' prior experience with FPV videos, 1 watched FPV videos more than once in the last 1 month, 6 about once a year, and 11 never. The participants received a nominal compensation for their participation.

doi:10.6342/NTU202303686

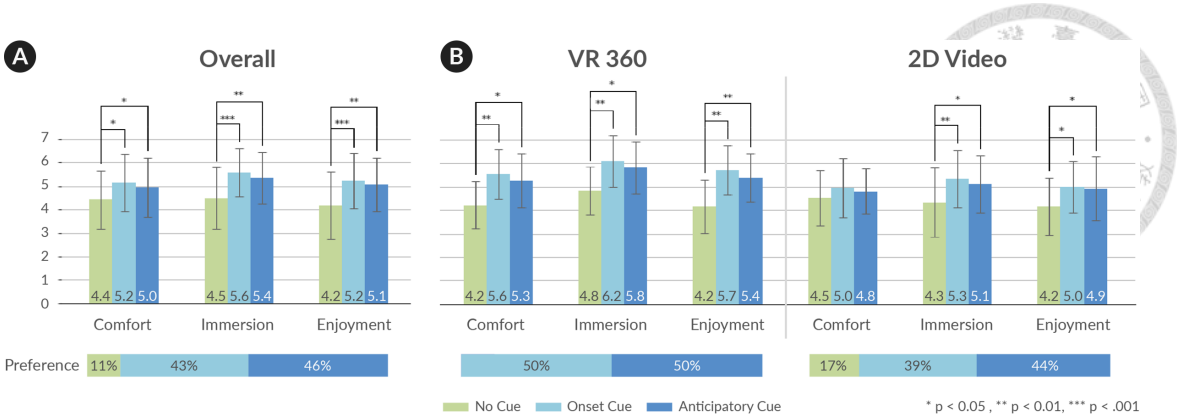

Figure 8.2: Average ratings of comfort, immersion, enjoyment on a 7-point Likert scale (with error bars showing standard deviation), as well as the distribution of the overall preference across three feedback conditions for: a) combined Overall results, and b) reported separately for VR 360 and 2D Video.

8.4 Results and Discussion

Figure 8.2(a) shows the overall average comfort, immersion, and enjoyment ratings on a 7-point Likert scale and overall preference across all 3 scenarios. Figure 8.2(b) separately shows results for VR 360 and for 2D Videos, which shows the average of both indoor and outdoor 2D videos. For Likert-scale ratings, effect size of each pairwise comparison is calculated as $r = \frac{Z}{\sqrt{N}}$ and interpreted using guidelines of 0.1 $\sim$ 0.3 (small effect), 0.3 $\sim$ 0.5 (moderate effect), and $\geq$ 0.5 (large effect) [29]. Friedman test showed significant difference among the cue designs for comfort, immersion, and enjoyment overall ($p < .05$). Two-tailed Wilcoxon matched-pairs signed-rank test with Bonferroni correction are used for pair-wise statistical significance.

Overall, participants rated both timing designs of TurnAhead to have significantly higher comfort (p = 0.0080 onset, 0.0118 anticipatory), immersion (p = 0.0003, 0.0007), and enjoyment (p = 0.0003, 0.0023) vs. the baseline, all with large effect sizes ($r \geq 0.5$). The average ratings are slightly higher for onset vs. anticipatory cues, though the differences were not statistically significant.

Looking at different scenarios, for VR 360, participants rated both onset and anticipatory cues to have significantly higher comfort (p = 0.0011, 0.0068), immersion (p = 0.0012, 0.0038), and enjoyment (p = 0.0005, 0.0023) for both timing designs compared

doi:10.6342/NTU202303686

to baseline, all with large effect sizes ($r \geq 0.5$). For 2D video, both timing designs had significantly higher immersion (p = 0.0005, 0.0038) and enjoyment (p = 0.0042, 0.0116) vs. baseline with large effect sizes ($r \geq 0.5$). However, although both timing designs had slightly higher comfort ratings vs. baseline, the differences were not statistically significant.

In terms of overall preference, 89% of the participants preferred TurnAhead, and among them, the timing preference was split with 48% preferring onset and 52% preferring anticipatory. For VR 360, all participants preferred TurnAhead, with an even split between onset and anticipatory. For 2D video, 83% of the participants preferred TurnAhead, and among them, the timing preference was split with 46% preferring onset and 54% preferring anticipatory.

Qualitative Feedback

During the pilot study, a participant whose research area is motion sickness in VR, exclaimed that the anticipatory cue provided the best FPV experience ever and was ”exciting” to use. More than half of the participants thought that anticipatory cue reduced their motion sickness because it let them know the direction of the next rotation in advance (P1, P3, P4, P5, P6, P7, P8, P9, P10, P11, P13, P15). Some reported that it helped them anticipate the cue of the *turning phase* which was at times too abrupt (P1, P4, P9, P10, P15). On the other hand, some found the anticipatory cue unreal (P11, P12, P15, P17) and was unnecessary for consecutive rotations with very short intervals (P0, P3, P10). A few participants felt that onset cue was more realistic because of the synchronization of viewpoint and actual head rotation (P2, P4, P7). Many participants reported that not knowing the direction of the next rotation in the no cue condition which lead to discomfort (P2, P4, P7, P8, P11, P13). However, a few participants preferred no cue for 2D video, because they were used to watching 2D video without haptic feedback, and felt weird when our device turned their heads forcibly (P10, P14).

doi:10.6342/NTU202303686

Chapter 9

Discussion and Future Work

9.1 Adaptive Anticipatory and Onset Cues

User experience evaluation showed split preference for anticipatory and onset cue (52% vs. 48%). Feedback showed that some preferred anticipatory cues for improved predictability of the next rotations, while some preferred onset cues for better synchronization of vestibular stimulation and visual perception, as well as the unpredictability which was more exhilarating.

The choice of anticipatory vs. onset can be adaptive to the content and the intended perception, and can even vary throughout a single FPV experience. For example, a FPV experience may start as a relaxing, cinematic overview of a theme park, using anticipatory cues, and then transition to an exciting segment that follows a roller coaster ride, using onset cues for less predictability and a more exciting viewing experience. We plan to explore the experience of combining and varying timing to better understand how it affects user experience.

9.2 General Model and Personalization

As the first exploration of using rotational cues for FPV experiences, we designed and evaluated a general model in our design process and studies. However, we observed split preference for anticipatory timing (600ms vs. 900ms) in Study 3 and anticipatory vs. onset

doi:10.6342/NTU202303686

in Study 4. Also, two users in Study 1 reported difficulty in recognizing cue directions even at the largest torque and longest duration, and some users in Study 2 reported the cue intensity being too high.

While the general model we designed serves as a good default setting, providing options to personalize timing and feedback intensity should further improve the experience. For example, providing the option to increase/decrease the intensity of cues should help improve cue recognition for some, while not being too strong for others (i.e. similar to how some games provide low/med/high options for game/FX sounds). Also, providing the option to select between 600ms, 900ms, and even adaptive timing based on rotation speed (e.g. longer timing for fast turns and shorter timing for slow turns).

9.3 Automating Rotation Analysis of FPV Videos

Automating FPV video analysis of rotations will help more content to become available for haptic feedback, by using our system and possibly with motion platforms. Although our survey of existing computer vision tools cannot fully automate the rotation analysis, optical flow analysis [23], which detects displacement of visual features, can partially help by inferring the direction and timing of rotation. While optical flow analysis cannot detect rotation angle/speed without depth information, we are exploring semi-automated analysis tools as well as evaluating ways to combine it with other automatic depth map generation techniques.

9.4 Comfort and VR Sickness

VR sickness occurs when the human brain receives contradictory sensory signals between visual and vestibular/body movement. User experience evaluation results showed that participants reported higher comfort ratings for TurnAhead in both scenarios, and the improvement was statistically significant ($p < .01$) for VR 360 but the improvement was not significant for 2D video. One possible reason is that VR 360 caused more discomfort than 2D videos, which is reflected in its lower comfort rating with no cue (4.2 vs. 4.5), thus

doi:10.6342/NTU202303686

the improvement was more noticeable.

FPV footage often use speed ramps in the editing process to speed up and slow down the video, resulting in apparent linear camera acceleration and deceleration. Speeding up is typically used in unimportant segment to speed up the tempo, while slowing down is used to allow the audience to pay attention and better observe what is going on around them. The speed ramps amplifies the inconsistency between the vestibular and visual systems, but the linear motion cues would need to be provided by systems such as HeadBlaster. To further improve the viewing experience of FPV, we are exploring designs that can provide lateral forces in 2-DoF and rotational forces in 3-DoF at the same time, that is, 5-DoF feedback.

doi:10.6342/NTU202303686

Chapter 10

Conclusions

We presented TurnAhead, which uses 3-DoF rotational haptic cues to improve the comfort, immersion, and enjoyment of FPV experiences. It uses headset-mounted air jets to provide ungrounded rotational forces that corresponds to camera rotation. We conducted a series of perception and formative studies to explore the design space of timing and intensity of haptic cues, followed by user experience evaluation, for a combined total of 44 participants. Results showed that both timing designs of TurnAhead, *onset* and *anticipatory*, significantly improved overall comfort, immersion, and enjoyment, and was preferred by 89% of participants. We are exploring personalize timing, content-based adaptive approaches, and 5-DoF feedback to further enhance the user experience.

doi:10.6342/NTU202303686

Bibliography

[1] K. Aoyama, H. Iizuka, H. Ando, and T. Maeda. Four-pole galvanic vestibular stimulation causes body sway about three axes. *Scientific reports*, 5(1):1–8, 2015.

[2] D. Artworks. Scifi platform city, mar 2022.

[3] H.-Y. Chang, W.-J. Tseng, C.-E. Tsai, H.-Y. Chen, R. L. Peiris, and L. Chan. Facepush: Introducing normal force on face with head-mounted displays. In *Proceedings of the 31st Annual ACM Symposium on User Interface Software and Technology*, pages 927–935, New York, NY, USA, 2018. ACM.

[4] J. Christensen. The quack attack is back, apr 2021.

[5] C. Diels and J. E. Bos. Self-driving carsickness. *Applied ergonomics*, 53:374–382, 2016.

[6] F. Gabbiani and S. Cox. *Mathematics for Neuroscientists*. Elsevier Science, USA, 2017.

[7] G. Gálvez-García, M. Hay, and C. Gabaude. Alleviating simulator sickness with galvanic cutaneous stimulation. *Human factors*, 57(4):649–657, 2015.

[8] J. F. Golding. Motion sickness susceptibility questionnaire revised and its relationship to other forms of sickness. *Brain research bulletin*, 47(5):507–516, 1998.

[9] J. Gugenheimer, D. Wolf, E. R. Eiriksson, P. Maes, and E. Rukzio. Gyrovr: Simulating inertia in virtual reality using head worn flywheels. In *Proceedings of the 29th Annual Symposium on User Interface Software and Technology*, pages 227–232, New York, NY, USA, 2016. ACM.

doi:10.6342/NTU202303686

[10] H. Gurocak, S. Jayaram, B. Parrish, and, and U. Jayaram. Weight sensation in virtual environments using a haptic device with air jets. *J. Comput. Inf. Sci. Eng.*, 3(2):130–135, 2003.

[11] S. Heo, C. Chung, G. Lee, and D. Wigdor. Thor's hammer: An ungrounded force feedback device utilizing propeller-induced propulsive force. In *Proceedings of the 2018 CHI Conference on Human Factors in Computing Systems*, pages 1–11, New York, NY, USA, 2018. ACM.

[12] M. Hoppe, D. Oskina, A. Schmidt, and T. Kosch. Odin's helmet: A head-worn haptic feedback device to simulate g-forces on the human body in virtual reality. *Proceedings of the ACM on Human-Computer Interaction*, 5(EICS):1–15, 2021.

[13] M. Israel. Airvūz, 2015.

[14] S. Je, H. Lee, M. J. Kim, and A. Bianchi. Wind-blaster: A wearable propeller-based prototype that provides ungrounded force-feedback. In *ACM SIGGRAPH 2018 Emerging Technologies*, pages 1–2. ACM, New York, NY, USA, 2018.

[15] B.-C. Ke, M.-H. Li, Y. Chen, C.-Y. Cheng, C.-J. Chang, Y.-F. Li, S.-Y. Wang, C. Fang, and M. Y. Chen. Turnahead: Designing 3-dof rotational haptic cues to improve first-person viewing (fpv) experiences. In *Proceedings of the 2023 CHI Conference on Human Factors in Computing Systems*, pages 1–15, New York, NY, USA, 2023. ACM.

[16] B. Keshavarz, B. E. Riecke, L. J. Hettinger, and J. L. Campos. Vection and visually induced motion sickness: how are they related? *Frontiers in psychology*, 6:472, 2015.

[17] Y. Kon, T. Nakamura, and H. Kajimoto. Hangerover: Hmd-embedded haptics display with hanger reflex. In *ACM SIGGRAPH 2017 Emerging Technologies*, pages 1–2. ACM, New York, NY, USA, 2017.

doi:10.6342/NTU202303686

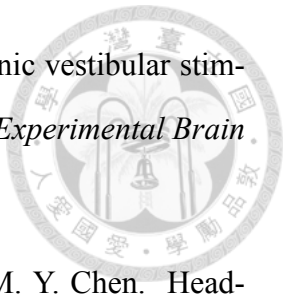

[18] B. Lenggenhager, C. Lopez, and O. Blanke. Influence of galvanic vestibular stimulation on egocentric and object-based mental transformations. *Experimental Brain Research*, 184(2):211–221, 2008.

[19] S.-H. Liu, P.-C. Yen, Y.-H. Mao, Y.-H. Lin, E. Chandra, and M. Y. Chen. Headblaster: a wearable approach to simulating motion perception using head-mounted air propulsion jets. *ACM Transactions on Graphics (TOG)*, 39(4):84–1, 2020.

[20] S.-H. Liu, N.-H. Yu, L. Chan, Y.-H. Peng, W.-Z. Sun, and M. Y. Chen. Phantomlegs: Reducing virtual reality sickness using head-worn haptic devices. In *2019 IEEE Conference on Virtual Reality and 3D User Interfaces (VR)*, pages 817–826, Osaka, Japan, 2019. IEEE, IEEE.

[21] N. A. Macmillan and C. D. Creelman. *Detection theory: A user's guide*. Cambridge University Press, UK, 1991.

[22] T. Maeda, H. Ando, and M. Sugimoto. Virtual acceleration with galvanic vestibular stimulation in a virtual reality environment. In *IEEE Proceedings. VR 2005. Virtual Reality, 2005.*, pages 289–290, Bonn, Germany, 2005. IEEE, IEEE.

[23] S. H. Park, B. Han, and G. J. Kim. Mixing in reverse optical flow to mitigate vection and simulation sickness in virtual reality. In *CHI Conference on Human Factors in Computing Systems*, pages 1–11, New Orleans, LA, USA, 2022. ACM.

[24] Y.-H. Peng, C. Yu, S.-H. Liu, C.-W. Wang, P. Taele, N.-H. Yu, and M. Y. Chen. Walkingvibe: Reducing virtual reality sickness and improving realism while walking in vr using unobtrusive head-mounted vibrotactile feedback. In *Proceedings of the 2020 CHI Conference on Human Factors in Computing Systems*, pages 1–12, New York, NY, USA, 2020. ACM.

[25] U. Pictures. Flying camera! ambulance fpv drone featurette, mar 2022.

[26] Porsche. Drive2extremes: Taycan cross turismo x johnny fpv, jun 2021.

doi:10.6342/NTU202303686

[27] A. Rolnick and R. Lubow. Why is the driver rarely motion sick? the role of controllability in motion sickness. *Ergonomics*, 34(7):867–879, 1991.

[28] J. M. Romano and K. J. Kuchenbecker. The airwand: Design and characterization of a large-workspace haptic device. In *2009 IEEE International Conference on Robotics and Automation*, pages 1461–1466, Kobe, Japan, 2009. IEEE, IEEE.

[29] R. Rosenthal, H. Cooper, L. Hedges, et al. Parametric measures of effect size. *The handbook of research synthesis*, 621(2):231–244, 1994.

[30] T. Sasaki, R. S. Hartanto, K.-H. Liu, K. Tsuchiya, A. Hiyama, and M. Inami. Leviopole: mid-air haptic interactions using multirotor. In *ACM SIGGRAPH 2018 Emerging Technologies*, pages 1–2. ACM, New York, NY, USA, 2018.

[31] M. Sra, A. Jain, and P. Maes. Adding proprioceptive feedback to virtual reality experiences using galvanic vestibular stimulation. In *Proceedings of the 2019 CHI conference on human factors in computing systems*, pages 1–14, New York, NY, USA, 2019. ACM.

[32] S. T. Flooded grounds, jan 2019.

[33] S. T. Sun temple, jan 2019.

[34] Y. Tanaka, J. Nishida, and P. Lopes. Electrical head actuation: Enabling interactive systems to directly manipulate head orientation. In *CHI Conference on Human Factors in Computing Systems*, pages 1–15, New York, NY, USA, 2022. ACM.

[35] Tesla. Flying through giga berlin, apr 2022.

[36] C.-Y. Tsai, I.-L. Tsai, C.-J. Lai, D. Chow, L. Wei, L.-P. Cheng, and M. Y. Chen. Airracket: Perceptual design of ungrounded, directional force feedback to improve virtual racket sports experiences. In *CHI Conference on Human Factors in Computing Systems*, pages 1–15, New York, NY, USA, 2022. ACM.

[37] C. Wang, D.-Y. Huang, S.-w. Hsu, C.-E. Hou, Y.-L. Chiu, R.-C. Chang, J.-Y. Lo, and B.-Y. Chen. Masque: Exploring lateral skin stretch feedback on the face with

doi:10.6342/NTU202303686

head-mounted displays. In *Proceedings of the 32nd Annual ACM Symposium on User Interface Software and Technology*, pages 439–451, New Orleans, LA, USA, 2019. ACM.

[38] Y.-W. Wang, Y.-H. Lin, P.-S. Ku, Y. Miyatake, Y.-H. Mao, P. Y. Chen, C.-M. Tseng, and M. Y. Chen. Jetcontroller: High-speed ungrounded 3-dof force feedback controllers using air propulsion jets. In *Proceedings of the 2021 CHI Conference on Human Factors in Computing Systems*, pages 1–12, New York, NY, USA, 2021. ACM.

[39] K. Watanabe, F. Nakamura, K. Sakurada, T. Teo, and M. Sugimoto. An Integrated Ducted Fan-Based Multi-Directional Force Feedback with a Head Mounted Display. In H. Uchiyama and J.-M. Normand, editors, *ICAT-EGVE 2022 - International Conference on Artificial Reality and Telexistence and Eurographics Symposium on Virtual Environments*, pages 55–63, Europe, 2022. The Eurographics Association.

[40] S. Weech, J. Moon, and N. F. Troje. Influence of bone-conducted vibration on simulator sickness in virtual reality. *PloS one*, 13(3):e0194137, 2018.

[41] S. Weech and N. F. Troje. Vection latency is reduced by bone-conducted vibration and noisy galvanic vestibular stimulation. *Multisensory Research*, 30(1):65–90, 2017.

[42] B. Yip and J. S. Jin. Determination of pivot point of a human head from the front. In *Proceedings of 2004 International Symposium on Intelligent Multimedia, Video and Speech Processing, 2004.*, pages 362–365, Hong Kong, China, 2004. IEEE, IEEE.

doi:10.6342/NTU202303686

Appendices

doi:10.6342/NTU202303686

Top 30 FPV Videos used in Rotation Analysis

Table 1: Links to the top 30 FPV videos analyzed in Section 2.

No.	Video
1	DJI FPV | A NEW WORLD
2	Madeira | Cinematic FPV
3	KOLD - My Best Drone Clips 2019
4	SANDSCAPE - Johnny FPV
5	6 Minutes Of Mountain Surfing in Norway | FPV Cinematics
6	Johnny FPV x Beautiful Destinations - Turkey
7	Cinematic FPV - Flying Over Switzerland
8	Drive2Extremes: Taycan Cross Turismo x Johnny FPV
9	Flying Through Giga Berlin
10	Right Up Our Alley
11	Topgolf FPV Venue Tour
12	Downtown Cinematic FPV
13	Morning Dives : Urban FPV
14	Formula 1, but in the streets of Miami...
15	American Muscle
16	DUBAI CHASING
17	Lucas Oil Interior // Final Four FPV
18	Good Morning America - Oscars After Party FPV Opener
19	The Quack Attack is Back
20	Music Festival FPV
21	Porsche Museum: The 30,000 Horsepower Aerial Drone Tour
22	Bowling Alley FPV Tour At Lightspeed
23	L'Automobile Paris - Cinematic FPV
24	Mercedes Benz Museum fly-through
25	Palazzo Farnese
26	One Take, Everybody Knows The Rules
27	Kudos Shanghai | FPV One Take
28	Envelopment
29	The Glensheen Experience
30	The National United States Airforce Museum FROM THE AIR!

doi:10.6342/NTU202303686

Line charts for the percentage of participants that recognized correctly in at least one of the two trials from Study #1

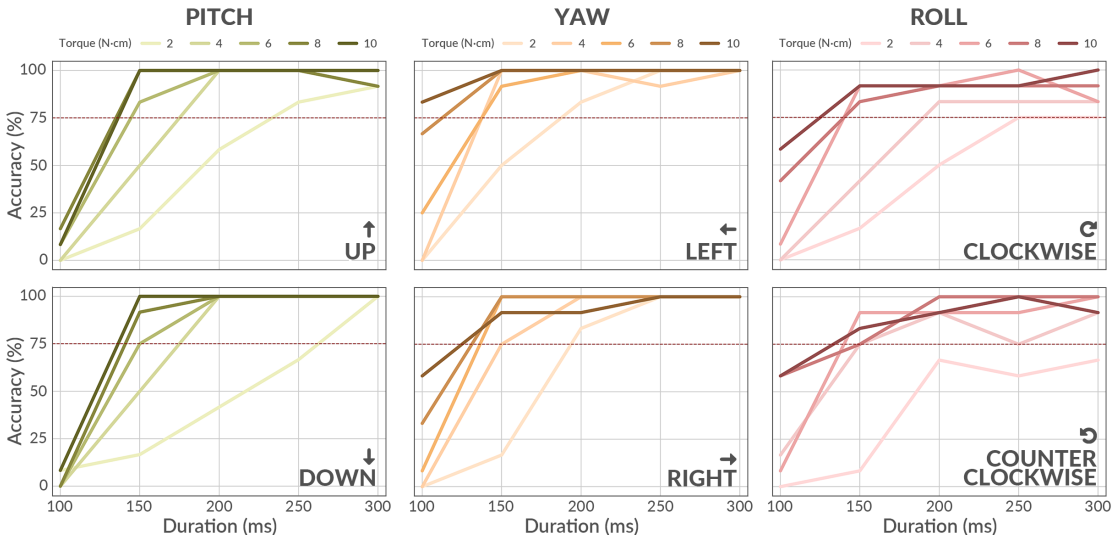

Figure 1: Percentage of participants that correctly recognized the haptic cue direction (in at least one of the two trials) vs. feedback duration and torque, for each of the 6 directions. The 5 lines in each chart are colored from light to dark to represent increase in torque. Horizontal red dotted lines indicate 75th-percentile accuracy (i.e. 75% recognition threshold).

doi:10.6342/NTU202303686